5-1-1982

Anatomy of the digestive system of Heliothis zea (Lepidoptera ; Noctuidae) larvae

M. W. MacGown

P. P. Sikorowski

Bulletin 905

May 1982

MITCHELL MEMORIAL LIBRARY
JUL 26 1982
Mississippi State University

Anatomy of the Digestive System of *Heliothis zea* (Lepidoptera; Noctuidae) Larvae

M. W. MacGown • P. P. Sikorowski

MAFES MISSISSIPPI AGRICULTURAL & FORESTRY EXPERIMENT STATION
R. RODNEY FOIL, DIRECTOR MISSISSIPPI STATE, MS 39762

Mississippi State University

James D. McComas, President Louis N. Wise, Vice President

Anatomy of the Digestive System of *Heliothis zea* Larvae

M. W. MacGown, Research Associate and
P. P. Sikorowski, Professor and Entomologist
MAFES/MSU, Department of Entomology

Acknowledgements

We extend our appreciation to the Mississippi State University Electron Microscope Center, Dr. Greta E. Tyson, Director, for assisting in numerous respects with this study. We also thank Drs. D. L. Bull, K. J. Judy, and J. P. Reinecke for critical review of the manuscript.

Anatomy of the Digestive System of *Heliothis zea* Larvae

Heliothis zea (Boddie) is a major pest of agricultural crops and is subject to extensive research. Several papers discuss the anatomy of this or related species, but a thorough anatomical treatment of the digestive system is lacking. Therefore, the anatomy of this species must be inferred from more inclusive studies.

Chauthani and Callahan (1967) first described the gross morphology, with corrections made later by Standlea and Yonke (1968). Chi et al. (1975) discussed the comparative morphology and histology of *Heliothis virescens* (F.), *H. zea* (Boddie) and *Spodoptera ornithogalli* (Guenee) and *S. frugiperda* (Smith) on the basis of gross dissection and light microscopy. Studies of *Hyalophora cecropia* by Judy and Gilbert (1969, 1970), traced the changes that occur during metamorphosis. Reinecke, Cook and Adams (1973), provide an excellent account of the hindgut musculature of *Manduca sexta;* Byers and Bond (1971), provide a topographic study of the hindgut of several species of Lepidoptera, including the Noctuidae, and Saini (1964) gave a concise anaysis of the cryptonephridial system of several superfamilies of beetles and of Lepidoptera.

Our study provides a comprehensive histological and topographical treatment of the digestive system, by means of light microscopy and SEM, of mature laboratory reared larvae of *H. zea* taken before the prepupal stage after feeding on artificial diet. This should lead ideally to developmental studies of each instar because a great many changes occur between and during molts, especially as the insect enters the prepupal stage.

Methods and Materials

Last instar larvae of *H. zea* were taken before the prepupal stage from cultures in our laboratory and were processed for histological observations or for scanning electron microscopy. A reasonable degree of uniformity was assured by dividing ten larvae from each rearing lot into two groups of five, for light microscopy and SEM. The procedures were repeated several times over a one-year period. Specimens used for light microscopy were killed and fixed by injection before storage in Bakers' formalin (Humason 1967) or Perfix® (Fisher Sci. Co.). Those fixed in Bakers' formalin (24 hr at room temperature) were processed (1) through 30-50-70-95% ethanol to absolute EtOH-Xylene and Xylene/paraplast 1:1, (2) to melted paraplast at 57°C and, infiltrated 2 hr under 30 cm vacuum and (3) were embedded. Dehydration fluids were changed three times each at 15 minute intervals.

Specimens fixed in Perfix were carried directly to 95% EtOH, and processed as those fixed in Bakers' formalin. The larvae were cut into sections of 1-3 segments long before dehydration to aid in rapid processing. Sections were cut at 2-10 μm on a rotary microtome, rehydrated, stained in Gill hemotoxylin No. 2 (Anon. 1976), dehydrated, counterstained in eosinated absolute ethanol, cleared and covered for observation. Most sections required destaining of the hematoxylin by 0.5% HCl. Extrusion vesicles of the midgut epithelium were subjected to the Feulgen reaction by following precisely the methods of Gurr (1962), using an eight minute hydrolysis period.

Specimens for SEM were killed and fixed by injection with either of the above agents. The larvae either were cut into three segments or the entire digestive systems were removed. These tissues were post-fixed in OsO_4 for four-to-seven hr, and were dehydrated through graded alcohols and immersed in three-to-five min changes of freshly opened absolute EtOH just before critical point drying with CO_2. The digestive systems were dissected on SEM stubs, were coated with gold on a Hummer II® sputtering device and were examined on a Hitachi HHS-2R® scanning electron microscope at an accelerating voltage of 20kV.

Photomicrographs were made on a Leitz Ortholux® microscope with Kodak Panatomic-X® film (ASA 32), a Nikon® camera back provided with automatic metering and shutter controls and with Tri-X-pan® 4x5 film in a Leitz Aristophot® bellows camera. Scanning electron micrographs were made on Polaroid® 55 film.

Descriptive Anatomy

Foregut (Figs 1-4)

Foregut consists of the buccal cavity, anterior and posterior pharynx, esophagus and crop, and terminates inside the anterior interstitial ring (AIR) of the midgut (Figs. 1-4). Epithelium of the buccal cavity is covered by a relatively thick intima. Various authors have cited specific dimensions for the thickness of the intima; but, in our experience, the thickness of both fore and hindgut intima is extremely variable. However, topographic features remain constant.

The intima of the buccal cavity is thoroughly covered with very fine, sharply pointed spicules as far back as the anterior pharynx. The anterior pharynx is a swollen area of the foregut that is convoluted in cross section and found anterior to the subesophageal ganglion. The food tube narrows above the subesophageal ganglion, with another dilation at the caudal end of the posterior pharynx. The entire pharynx bears small caudally directed spicules that are stouter than those of the buccal cavity, but they are not easily visualized in light microscopy because of the irregularities of the intima.

The esophagus originates at the end of the last internal lobe of the posterior pharynx and extends back to the crop. It consists of a very flat epithelium with widely spaced nuclei closely flattened against the intima. The esophagus widens at the crop, and there is no clear distinction between the two.

The epithelium of the crop remains flattened against the intima, and cell borders of both crop and esophagus are obscure (Fig. 4). The crop extends, apparently unmodified, into the anterior opening of the midgut and terminates inside the first plica of the midgut.

The transition from foregut to midgut is marked clearly by the narrow band of cells of the AIR, composed of cuboidal epithelium with large nuclei closely packed against the cell membranes. A similar series of cells occurs at the posterior end of the midgut. The musculature of the anterior and posterior pharynx is well veloped, consisting of stout circu and longitudinal muscles and t dorsal and ventral dilators of t pharynx.

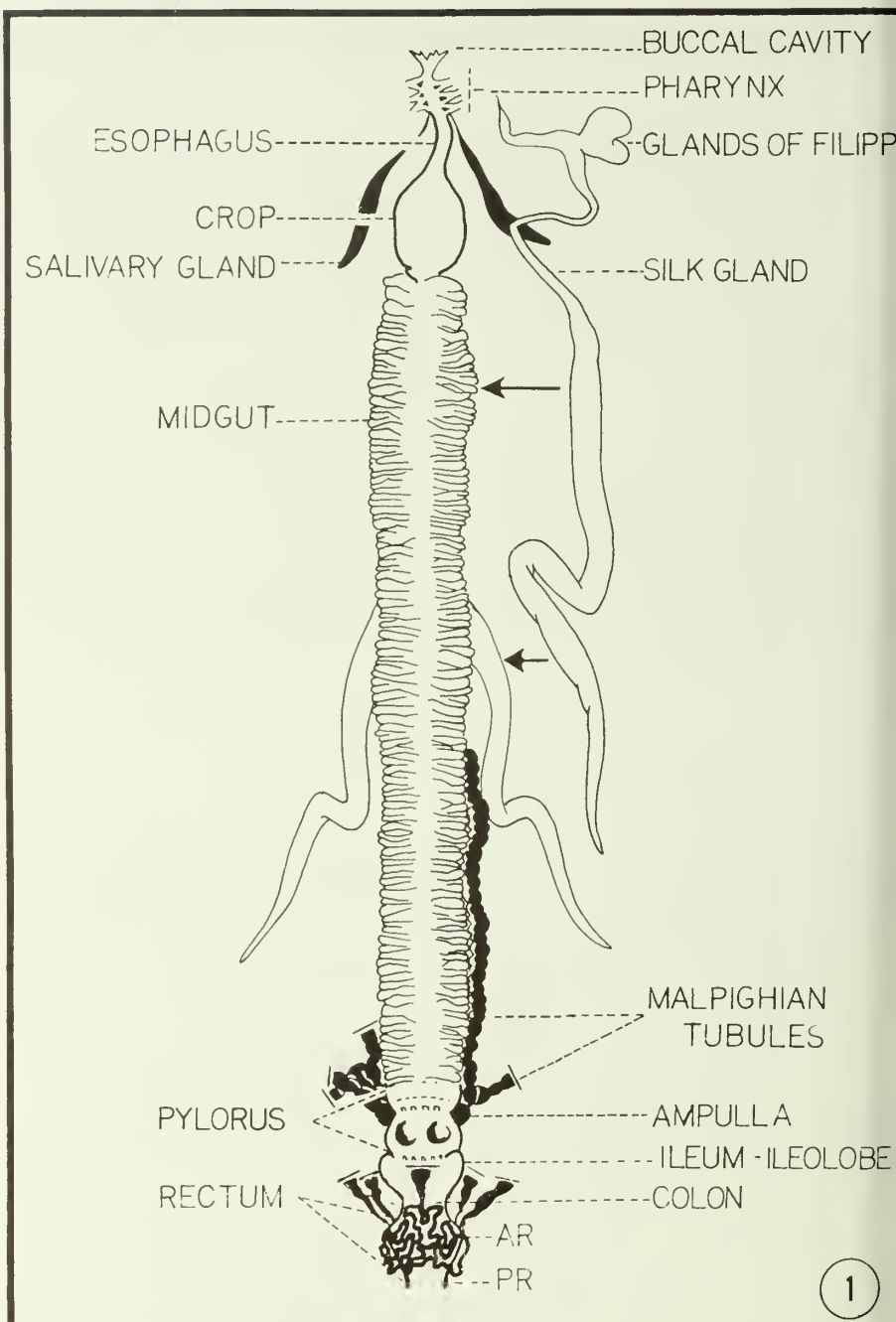

Figure 1. Generalized diagram of *Heliothis zea* larval digestive system, drawn and reduced from a large composite scanning electron micrograph. AR, anterior rectum, PR, posterior rectum.

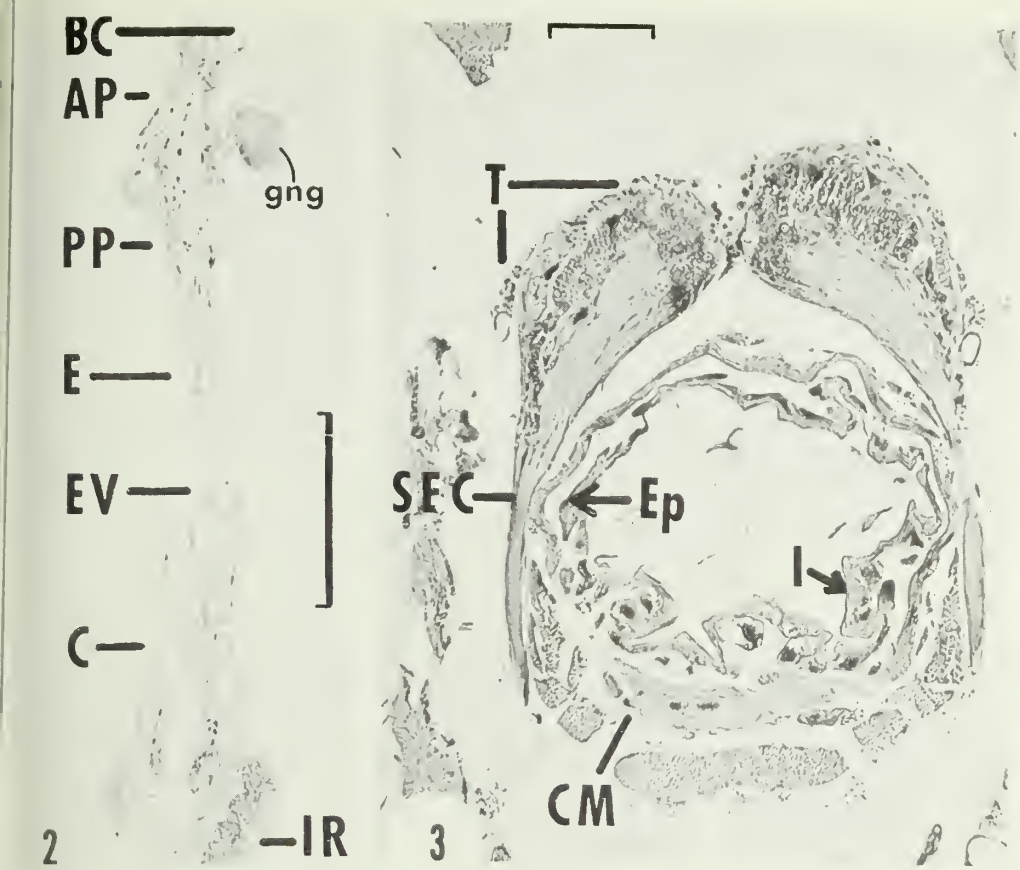

Figure 2. Overview of foregut in sagittal section. AP, anterior pharynx; BC, buccal cavity; C, crop; E, esophagus; EV, esophageal valve; IR, interstitial ring of anterior midgut; gng, ganglion. Bar = 500 μm. Figure 3. Transection of pharynx at tritocerebrum. CM, circular muscle; Ep, epithelium; I, intima; SEC, subesophageal connective; T, tritocerebrum. Bar = 100 μm. Figure 4. Sagittal section through crop. AIR, anterior interstitial ring; Ep, epithelium (extremely flattened); I, intima; L, lumen; MG, midgut. Bar = 100 μm.

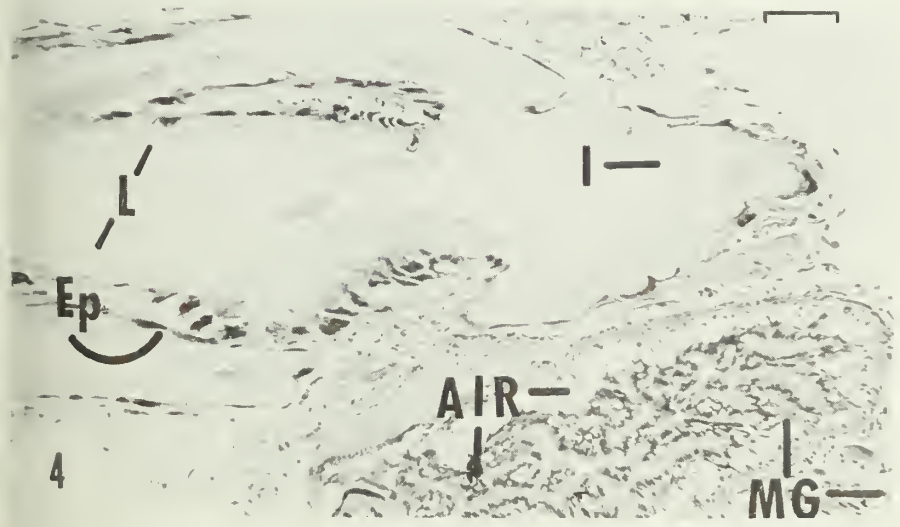

Midgut (Figs. 5-14, 24)

The midgut consists of a long tube of epithelial cells bound by a basement membrane and circular and longitudinal muscles and originates at the anterior interstitial ring. The midgut is incised transversely by constrictions that throw the epithelium into regular folds (Figs. 5, 24), each consisting of a number of goblet cells with large interior cavities and adjacent columnar cells (Figs. 12-14). The columnar cells are very narrow and are compressed between the goblet cells so that they appear to be a majority of the latter; however, this is misleading and there are at least four columnar cells per goblet cell; and the columnar cells account for the striated border of the epithelium.

Goblet cell cavities appear mainly in the upper 1/2 of the cell, the nuclei below (Fig. 24). The cavities vary from about 18-35 μm long and 7-10 μm across and contain microvilli about 2 μm long and 0.25 μm broad (Figs. 13, 14).

The post-digestive processes are marked by extrusion of vesicles from the cells into the lumen (Figs. 6-11, 24). The vesicles give a negative Feulgen reaction but retain Gill hematoxylin in regressive staining. The literature appears vague as to the identity of these extrusion bodies; i.e., whether they are packets of cellular breakdown products, contain enzymatic substances that digest the food or are extruded nuclei from degenerating epithelial cells. Regressive staining by hematoxylin suggests nuclei because the vesicles retain the stain well. However, the Feulgen-schiff reac-

tion is negative, hence the absence of DNA is demonstrated.

Specific enzymatic tests were not performed, but the great increase in extrusion vesicles after digestion, especially before and entering the prepupal stage, suggests that the vesicles are probably cellular breakdown products released into the gut lumen and that the enzymatic release probably occurred as secretion from the epithelium much before the development of the vesicles. This seems much more plausible, especially since there is no way that the vesicles could penetrate the peritrophic membrane. Thus, in this view, what appears to be merocrine secretion is suggested to be the release of cell breakdown products after digestion (in the form of the extrusion vesicles).

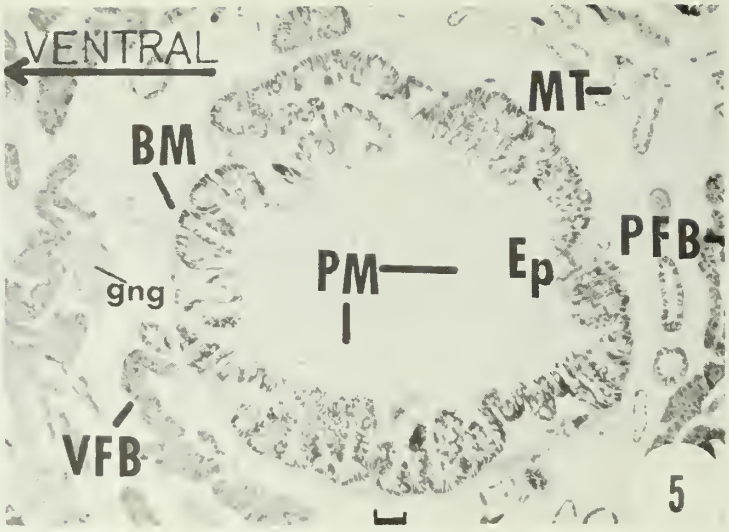

Figure 5. Transection through midgut tissues near anterior end, showing the characteristic folded structure. BM, basement membrane; Ep, epithelium; gng, ganglion, MT, Malpighian tubules; PFB, peripheral fat body; PM, peritrophic membrane; VFB, visceral fat body. Bar = 100 μm.

The vesicles emerge through the striated border, perhaps as a result of mechanical pressure induced by

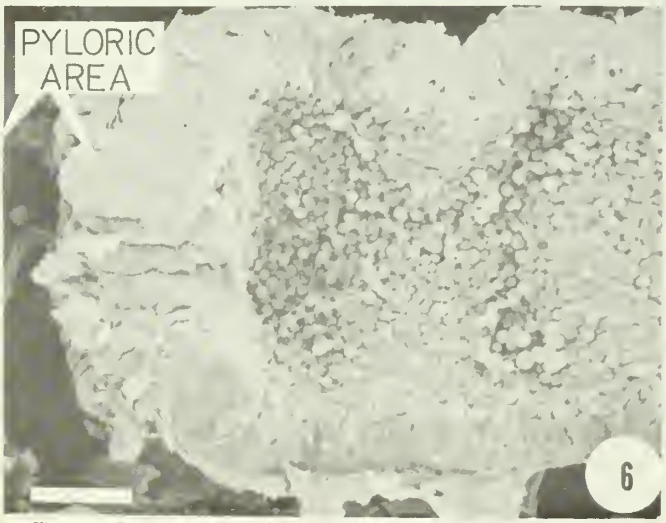

Figure 6. Sagittal section of midgut at the pyloric cone, showing a large number of extrusion vesicles as well as 2 shapes of midgut epithelial cells (elongate, lobed cells on right). Bar = 100 μm.

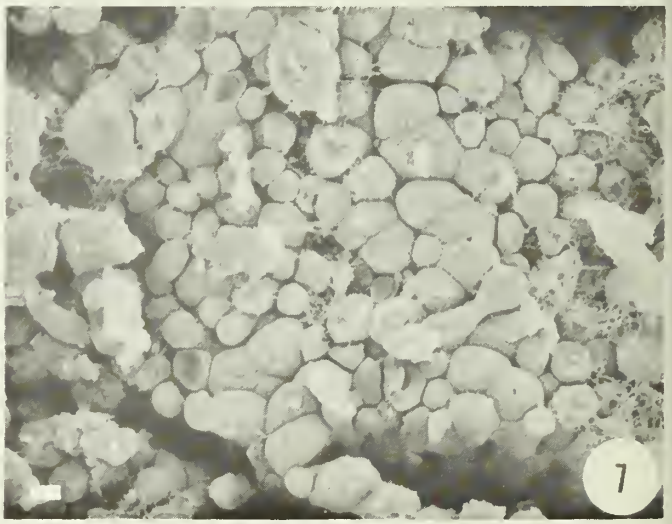

Figure 7. Close view of midgut epithelial surface showing extrusion vesicles, turgid and exploded cells, and surface debris. Bar = 10 μm.

Figure 8. Enlarged view of epithelium showing a newly emerging extrusion vesicle (V.). Bar = 10 μm.

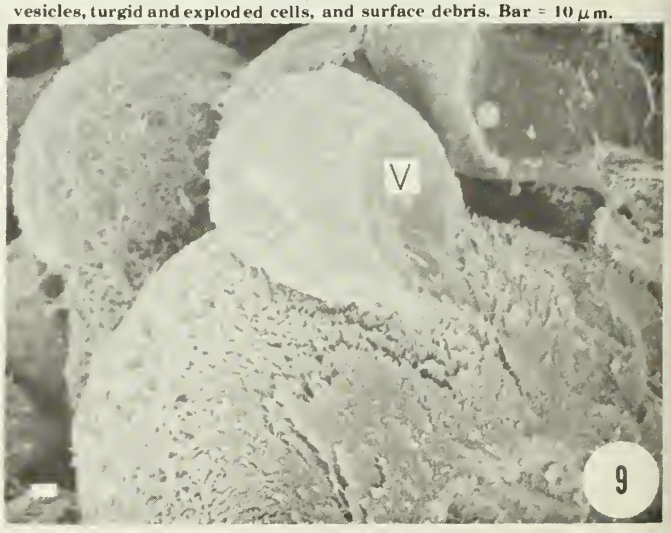

Figure 9. Extrusion vesicle protruding through the surface of an epithelial cell. These vesicles appear to be covered with a membrane upon emergence, although this was not demonstrated histoologically. Bar = 1 μm.

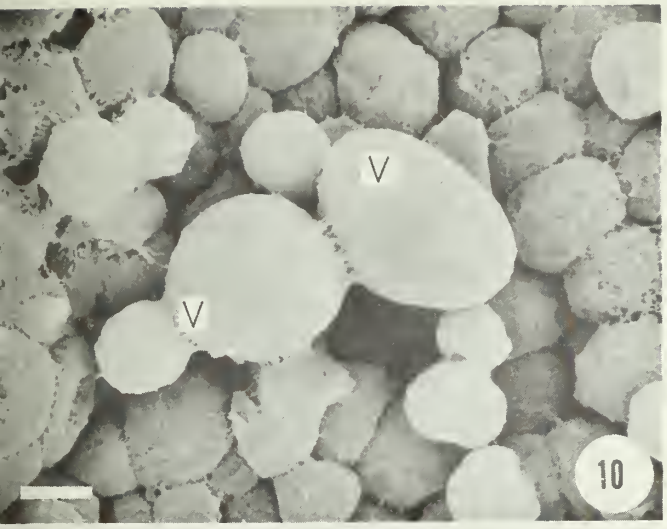

Figure 10. Coalescence of vesicles (V). Bar = 10 μm.

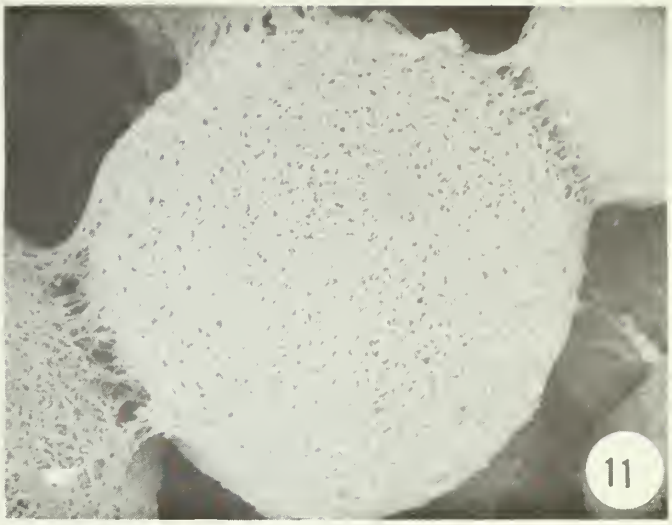

Figure 11. Spongy surface of mature, emerged vesicles, and coalescence. Bar = 1 μm.

regenerative cells below or because of changes in osmotic pressures. Tears are evident in the cell membranes as the vesicles enlarge (Fig. 9), and the vesicles completely emerging from the cell, appear to be enclosed in a membrane (not demonstrated by histology). At a later stage, the vesicles develop a spongy, mesh-like appearance, begin to coalesce with neighboring vesicles and cover the epithelial surface of the midgut (Figs. 10, 11).

Midgut and hindgut are separated at the posterior interstitial ring, which is composed of cuboidal epithelium like that of the anterior interstitial ring (Fig. 25). The ring merges into the intima and produces cells in the first plica of the pyloric cone (Fig. 18).

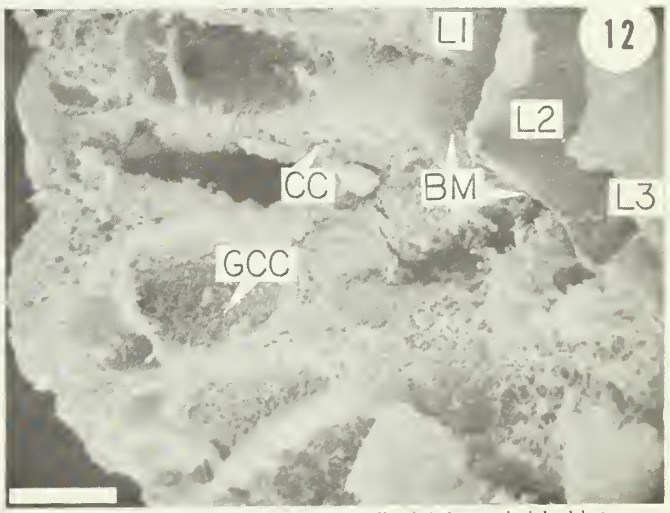

Figure 12. Goblet cells, with columnar cells tightly sandwiched between. Basement membrane separates into 3 lamellae (L1, L2, L3), the first appearing to be a condensation of the bases of the epithelial cells. Pores are seen through the tops of the goblet cells. Their function is not clear, but they may be associated with the extrusion vesicles seen in Fig. 13. CC, columnar cells; GCC, goblet cell cavity; BM, basement membrane. Bar = 10 μm.

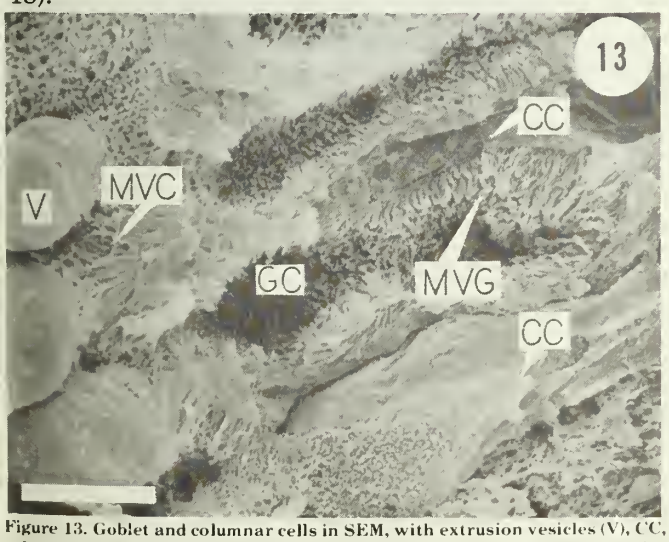

Figure 13. Goblet and columnar cells in SEM, with extrusion vesicles (V), CC, columnar cell; GC, goblet cell; MVC, microvilli of columnar cell; MVG, microvilli of goblet cell; V, vesicle. Bar = 10 μm.

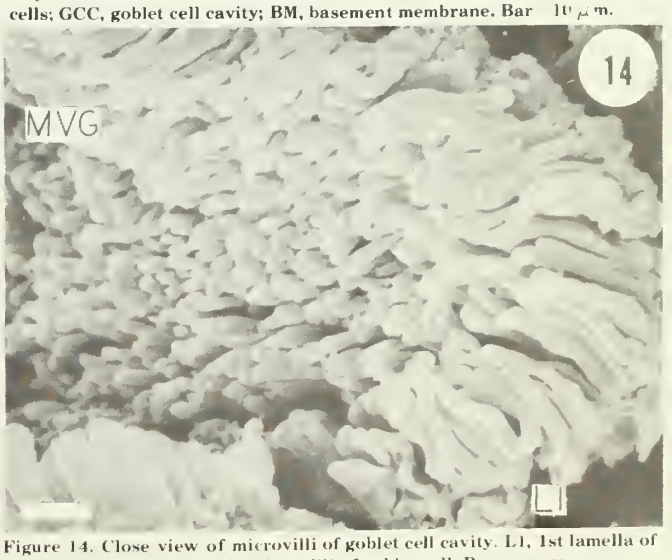

Figure 14. Close view of microvilli of goblet cell cavity. L1, 1st lamella of basement membrane; MVG, microvilli of goblet cell. Bar = μm.

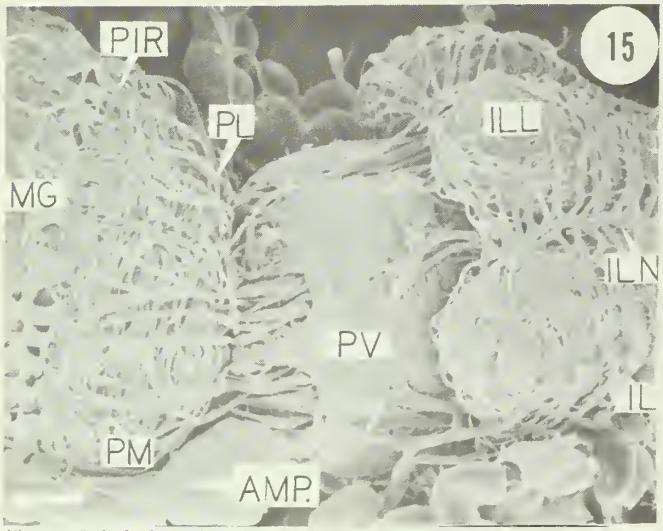

Figure 15. Pyloric region; dorsal view in SEM, showing orientation of the midgut, pyloric cone, pylorie valve, and ileum. Bar = 100 μm. (See Fig. 16 for abbreviations).

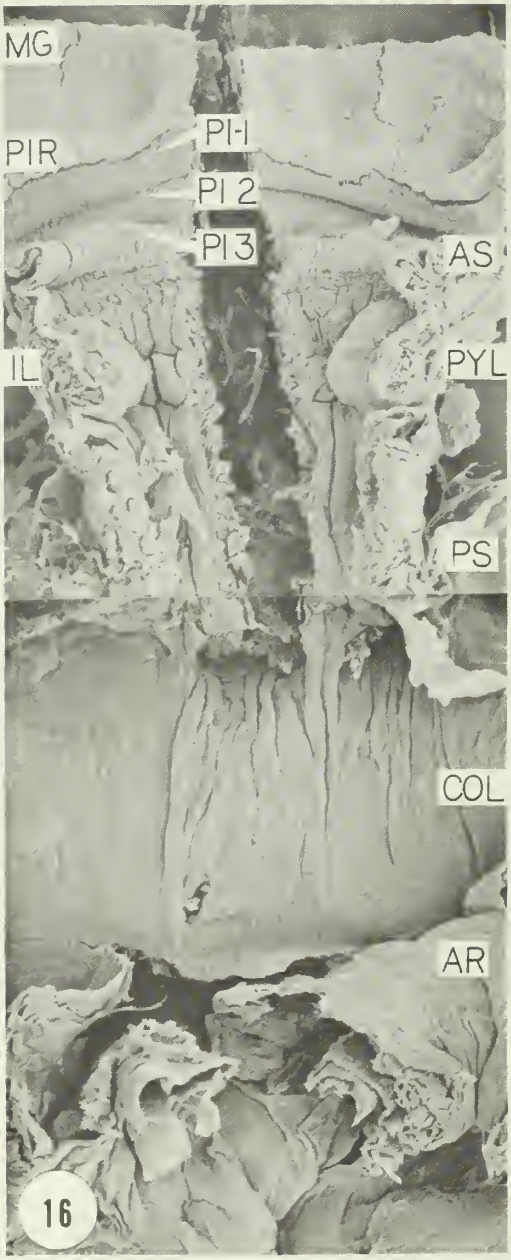

Figure 16. Pyloric region, ileum, colon and anterior rectum split longitudinally to show intern organization. (Approx. same scale as Fig. 15). AR, anterior rectum; AS, anterior sphincter; CO colon; IL, ileum; ILL, ileolobe; ILN, ileonode; MG, midgut; PIR, posterior interstitial ring; PI- 1st plica; PI-2, 2nd plica; PI-3, 3rd plica; PM, pyloric cone circular muscles; P3, posteri sphincter; PV, pyloric valve; PYL, pylorus.

Hindgut (Figs. 1, 15-23, 25-49)

Hindgut comprises the pyloric cone, pylorus, ileum, colon and rectum (Figs. 15-17). The pyloric area is by far more difficult to interpret than is any other area of the digestive system, because it may be distended or contracted so as to obscure some of its features. However, distinctive areas may be shown topographically. The hindgut is seen from the outside to originate at the posterior interstitial ring (PIR), indicated by a muscular halter (Fig. 15). The PIR marks the beginning of intima producing epithelium (Fig. 18,19). The area between the PIR and the tightly compressed anterior sphincter is the pyloric cone, which is covered by dense circular and longitudinal muscles. Posterior to this is a short pyloric valve. Overlying the pyloric value posteriorly are six ileolobes, which are large muscular extensions of the ileum that project forward over the base of the pyloric valve. The ileolobes terminate caudally in the ileum, closed by the posterior sphincter, which opens into the colon (Figs. 16, 17). The colon may be swollen or not, depending upon the presence of a fecal pellet, and opens into the anterior rectum by a muscular sphincter without internal differentiation.

Pylorus

The posterior interstitial ring immediately precedes the first plica of the pylorus. The cuboidal cells of the PIR (Fig. 25), when subjected to Feulgen reaction, gave results the same as those regressively stained by Gill hematoxylin-eosin.

Three major plicae follow the PIR and are identifiable by their spicules (Fig. 17). The first plic bears transverse rows of caudall projecting spicules (10 μm long 0.2 μm across the base), set withi small folds of intima (Figs. 31, 32 Plica two bears sparse, caudall directed spicules about 3 to 4 μm long and 0.1 μm across the bas (Fig. 33) and merges into wrinkled, third fold Pl-3, wit

parse spicules about 2 μm long nd 0.4 μm across the base. They re oriented caudad or cephalad lepending on the wrinkles of the ntima (Fig. 34, 35).

Internal lobes project into the umen at the pyloric-ileal junction, nd consist of clusters of epithelial ells covered with a thick, spiny ntima (Figs. 17, 20, 36, 37). These obes are unusual because the spicules point forward toward the pylorus. Each lobe is composed of subunits of two to three cells that form smaller lobes (Fig. 20). The epithelium consists of large cells, 100 to 130 μm-long, that contain elongate to lobed nuclei. Short, transverse bundles of muscle fibers occur between the smaller lobes. Cell membranes are usually indistinct. The deep, spiny intima appears to shred the peritrophic membrane as it passes into the ileum (Figs. 21, 37).

Ileum

The ileum consists of six ileolobes, which are large extensions of the ileum that project forward over the pyloric valve anteriorly, and a narrower neck that opens into the colon via the posterior sphincter (Fig. 17). The intima consists of thick oval humps protruding into the lumen at the ilelobes, longitudinally folded intima of the neck or tubular region (Fig. 38) and caudally directed spicules of the posterior sphincter (Fig. 39).

Internal nodes in each ileolobe occur in apposition to each other (Figs. 22, 23). Circular muscles occur between the ileum and ileolobe, and a ring of circular muscle enevelops both. Epithelial cells have indistinct cell membranes and small rounded nuclei. Ileonodes have giant epithelial cells in the apical region and smaller cells basally (Fig. 22). Intima of the lobes, nodes and ileum are variable in thickness --- thin and imperceptible in some

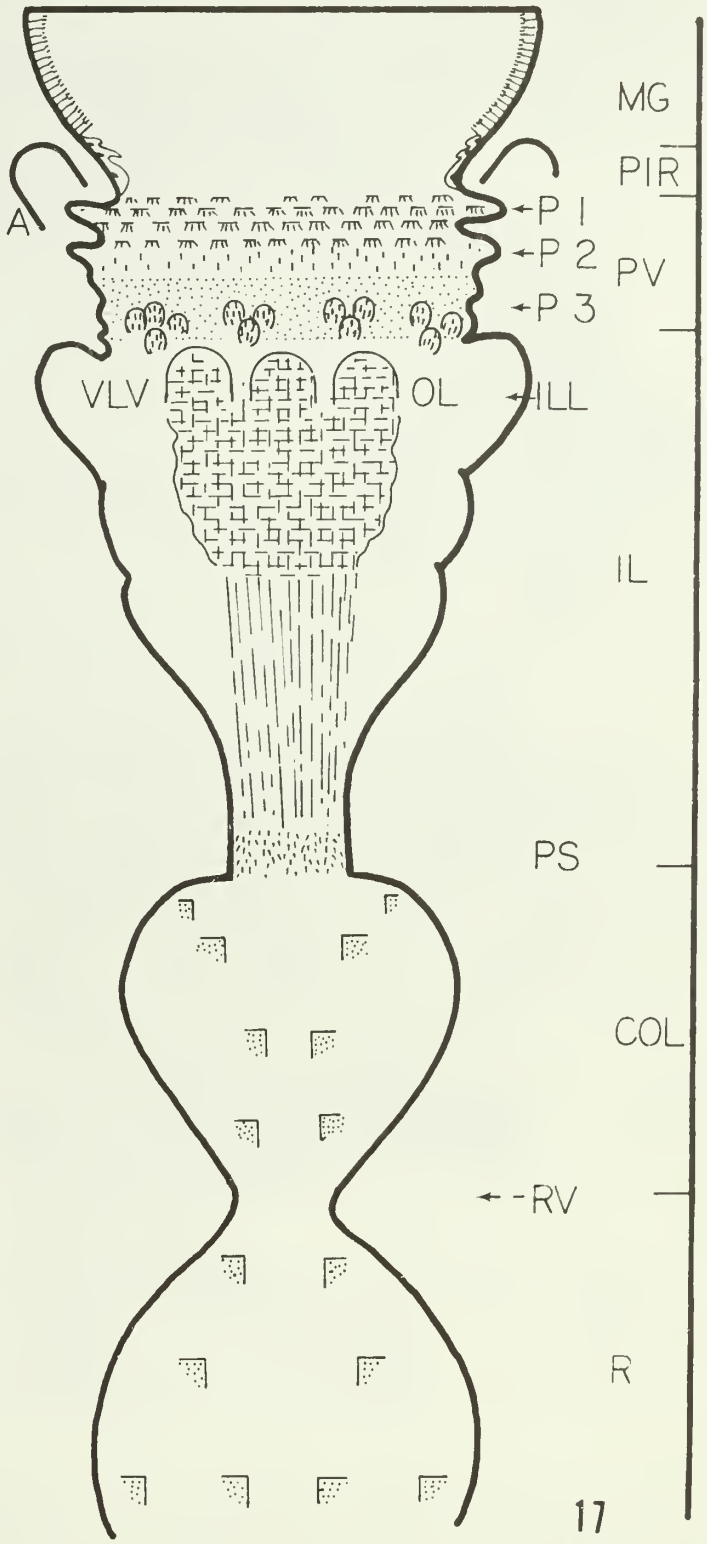

Figure 17. Diagrammatic map of hindgut topography. A, Ampulla of Malpighian tubules; COL, colon; IL, ileum; ILL, illeolobe; MG, midgut; OL, occluding lobe of ileum; P-1, 1st plica of pyloric cone; P-2, 2nd plica of pyloric cone; P-3, 3rd plica of pyloric cone; PIR, posterior interstitial ring; PS, posterior sphincter of ileum; PV, pyloric valve; R, rectum; RV, rectal valve; VLV, valvulae of anterior sphincter (P1-3) of pylorus.

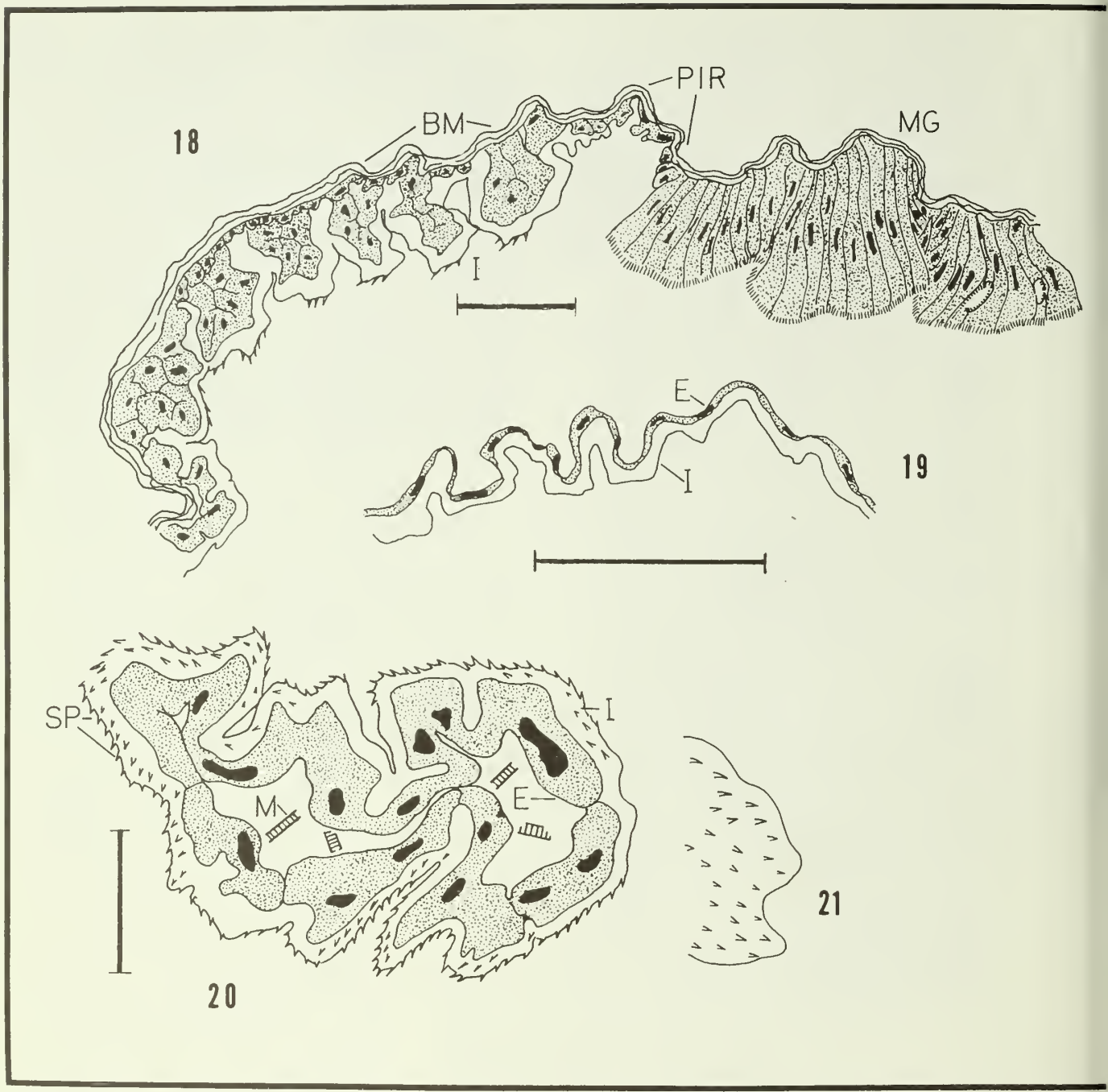

Figure 18. Diagrammatic longitudinal section at junction of midgut and hindgut, marked by posterior interstitial ring. First plica of pylorus with caudally directed spicules succeeds the ring. BM, basement membrane; I, intima; Mg, midgut; PIR, posterior interstitial ring. Bar = 100 μm. Figure 19. Close view of intima producing ring. Bar = 100 μm.

Figure 20. Transverse section through valvula of pyloric-ileal junction; 2- cells form subunits of the valvulae; epithelium with very large cells, indistir borders, large, lobed nuclei and thick, spiny intima. I, intima; E, epitheli cell; M, muscle; SP, spicules. Bar = 100 μm. Figure 21. Inset-enlargement o intima in Fig. 20.

specimens, very thick and fluted in others. Thick, fluted epithelium occur in the enlargement of apposed ileonodes (Fig. 23). Paired tracheae occur at the junction of the ileonodes and ileum. Other authors have noted that ileonodes similar to these occur between the ileolobes --- i.e., the depression occurring between the enlarged nodes (Fig. 15). The nodes in *H. zea* occur within as well as between lobes and, in the lobed and tubular regions of the ileum. Spiculate lobes at the pyloric-ileal junction of the intima of Pl-3 may be found farther back into the ileum if th gut is distended (full) or at th posterior margin if withdraw (empty); therefore, the true origin o the ileum may not at first b evident. The valvulae themselve can be interpreted as marking th origin of the ileum internally.

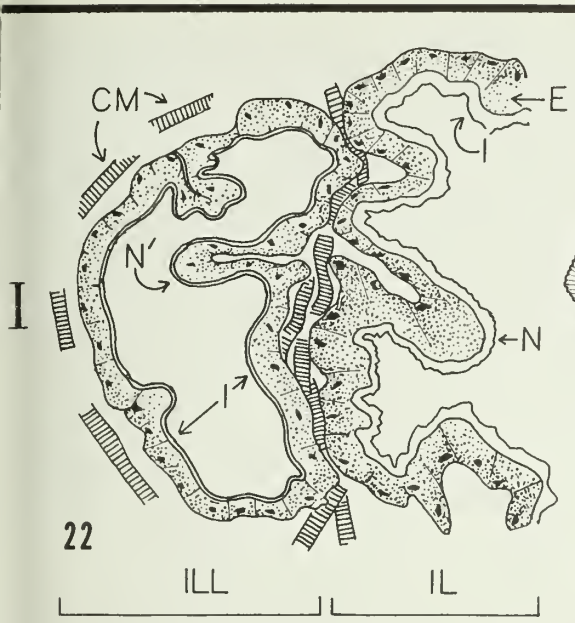

Figure 22. Transection of ileum and one ileolobe. Nodes (N, N') project into the lumen of the ileum and ileolobe. The intima of such nodes varies from very thin to thick and fluted. Epithelial cell borders are for the most part obliterated, and giant cells occur toward the apex of the nodes. CM, circular muscle; E, epithelium; I, intima; N,N', nodes of ileum. Bar = 100 μm. Figure 23. Enlargement of the nodes (N,N') projecting into the lumen of the ileum and ileolobe. The large "giant cells" occur near the apex. Intima may have a deeply fluted appearance over these nodes, less so over the rest of the epithelium. CM, circular muscle; ILL, ileolobe; N, node of ileum; N', node of ileolobe; TR, tracheae. Bar = 100 μm.

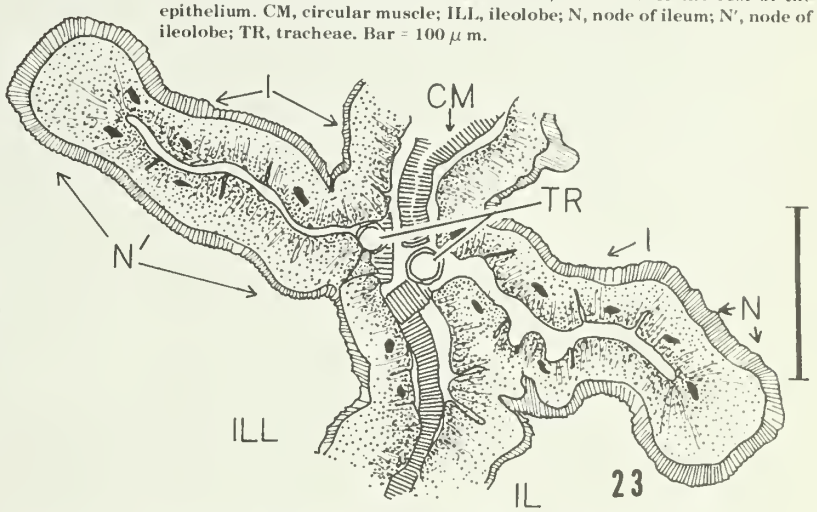

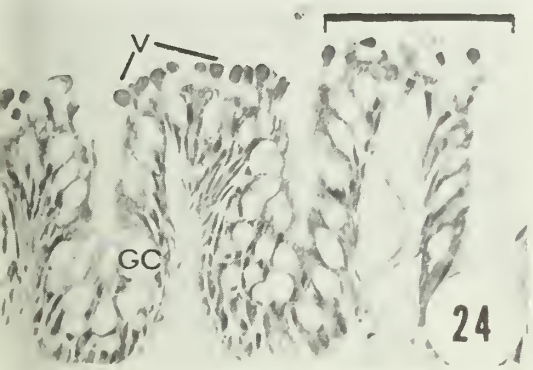

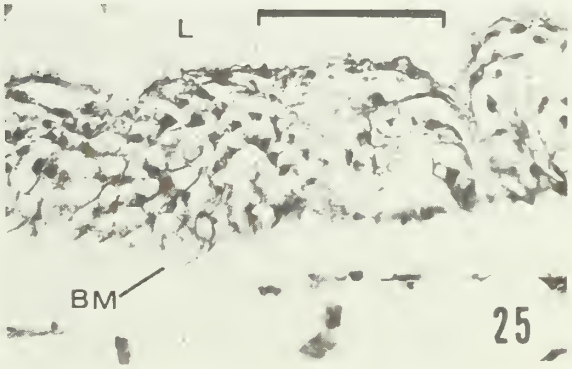

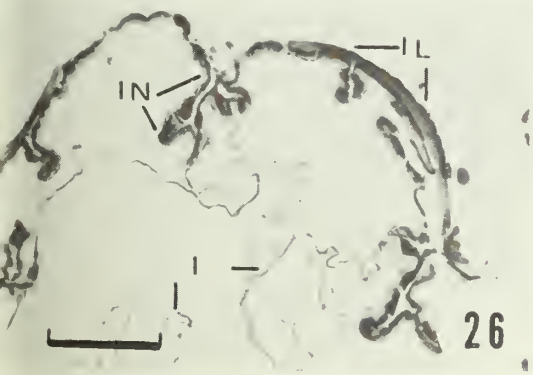

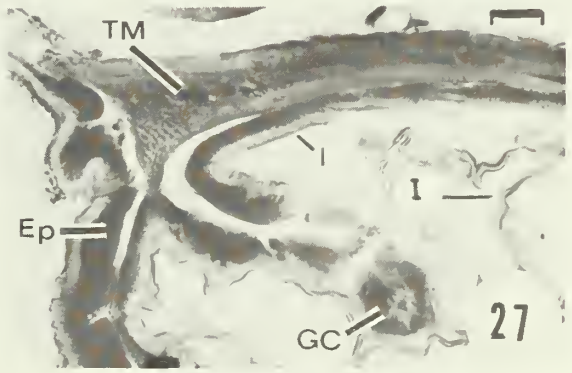

Figure 24. Folds of midgut epithelium showing extrusion vesicles; vesicles stain heavily with Gill hematoxylin but give negative Feulgen reaction. GC, goblet cavity; V, vesicles. Bar = 70 μm. Figure 25. Transection through posterior interstitial ring (PIR). AIR is essentially the same. BM, basement membrane; L, lumen. Bar = 70 μm. Figure 26. Ileolobes and nodes, transection through ileum. IL, ileolobe; IN, ileonode; I, intima. Bar = 100 μm. Figure 27. Attachment of transverse muscles to epithelium of the ileonodes and adjacent lobes. Ep, epithelium; GC, giant cell; I, intima; TM, transverse muscle. Bar = 10 μm.

Colon

The ileum empties into the colon via the posterior sphincter, a short series of cells with caudally projecting spicules (Fig. 39). The colon is distinguishable by the epicuticular depressions, made up of minute crater like impressions of the intima that are visible at 4000 X or more (Figs. 46-48). The intima of the colon, rectum and anal membranes is entirely and finely dotted with these structures. The epicuticular depressions in certain specimens appear to be perforations (Fig. 48), but in others appear to be closed and very uniform in size and shape.

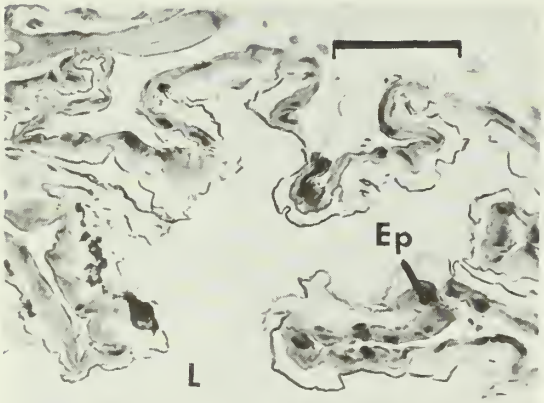

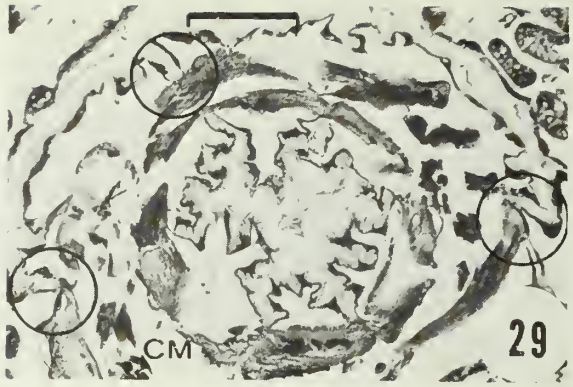

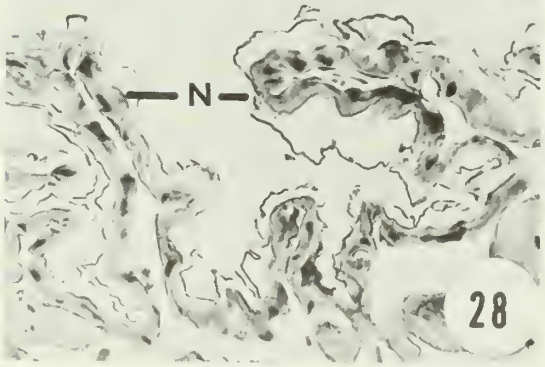

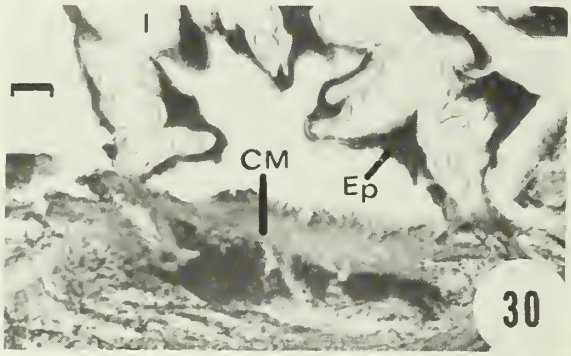

Figure 28. Higher magnification of ileal cross section from Fig. 26, with thick intima, numerous secondary infoldings. Ep, epithelium; L, lumen; N, nodes of ileum. Bar = ca. 50 μm. Figure 29. Cross section of colon at hinge points of perinephric membrane. Colon epithelium attaches at 6 distinct points to the circular muscle, preserving the 6-lobed pattern of the anterior ileum. Encircled areas show hinges of membranes of cryptonephridic system. CM, circular muscle. Bar = 100 μm. Figure 30. Close up of attachment of colon epithelium to transverse muscle. Intima is produced to displace epithelial cells, forming a stout bond to muscle. Ep, epithelium; CM, circular muscle. Bar = 10 μm.

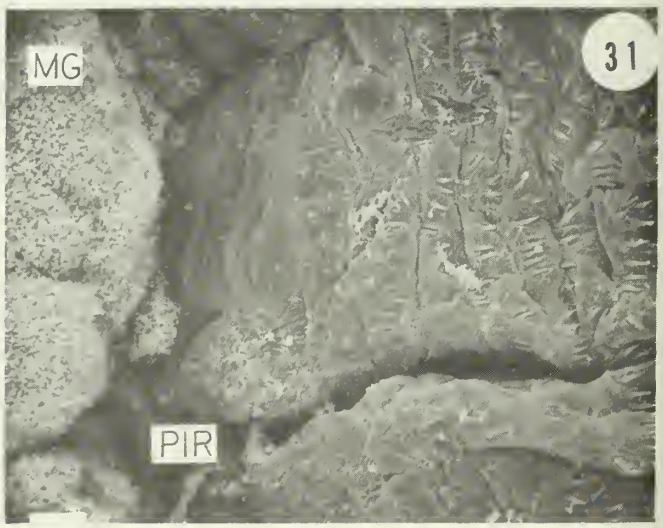

Figure 31. Juncture of midgut and 1st plica of pyloric cone, with backward projecting setulae and deeply infolded PIR. MG, midgut; PIR, posterior interstitial ring (infolding of surface). Bar = 10 μm. Figure 32. Enlargement of 1st plica of pyloric cone, PL-1. Bar = 10 μm.

Rectum

The colon (Figs. 29, 30, 40-45) empties into the anterior rectum through a simple muscular sphincter, the rectal valve, without differentiation of the intima. Anterior rectum is identifiable by the cryptonephridial arrangement of the Malpighian tubules, i.e., a double layer of tubules in the anterior rectum and no tubules in the posterior. The anal region maintains the six-plicate pattern of the remainder of the hindgut (Fig. 49) and is dotted with epicuticular depressions.

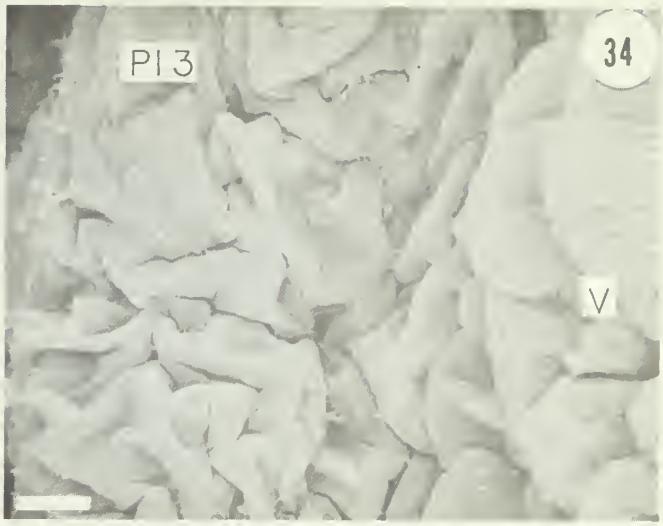

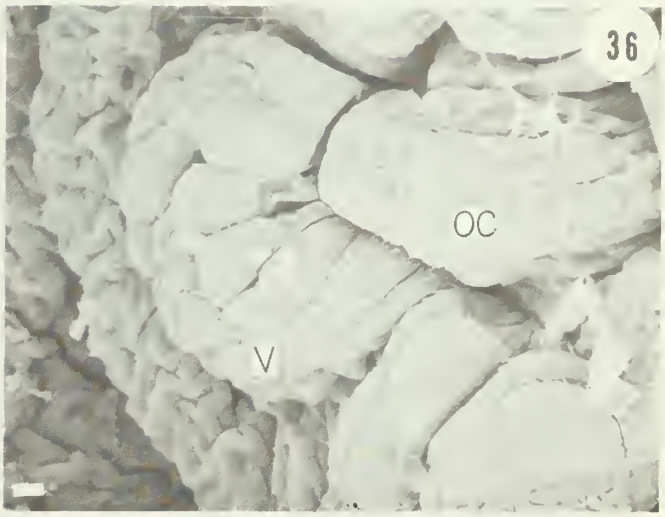

Figure 33. Second plica of pyloric cone, with sparse setulae. Bar = 10 μ m. Figure 34. Third plica and valvulae (V) of pyloric cone. Valvulae belong to the anterior sphincter of the pylorus. Bar = 10 μ m. Figure 35. Enlarged view of setulae of 3rd plica (Pl-3). Bar = 1 μ m. Figure 36. Third plica, merging with valvulae (V) and occluding lobes (OC) of the anterior sphincter. The latter two structures occur at the beginning of the ileum. Bar = 10 μ m.

Figure 37. Spicules of the valvulae found at the pyloric-ileal junction. The setulae project cephalad. Bar = 10 μm. Figure 38. Post valvular intima of epithelium, consisting of blocky to convoluted texture, creased longitudinally. Bar = 1 μ m.

Malpighian tubules

Malpighian tubules originate at the pylorus as two ampullae, one on either side and each with a major branch that divides into three elongate tubules. The six tubules progress forward 1/2 to 2/3 the distance of the midgut, turn and run back to the ileum, then become highly convoluted over the ileum and closely packed in a mass known as the iliac plexus. They emerge from this, and two enter the anterior rectum dorsally, two laterally and two ventrally, progress caudad to the posterior rectum, then through a double membrane, turn and proceed cephalad, then bend again caudally. The cryptonephridial system of *H. zea* conforms to that described by Saini (1964). The rectal chamber may be either collapsed (Figs. 40, 44) or distended (Figs. 41, 45) but shows the cryptonephridial system most clearly when distended.

Figure 39. Posterior ileal sphincter, with caudally directed setulae forming a narrow band around the ileo-colon junction. Bar = 10 μm.

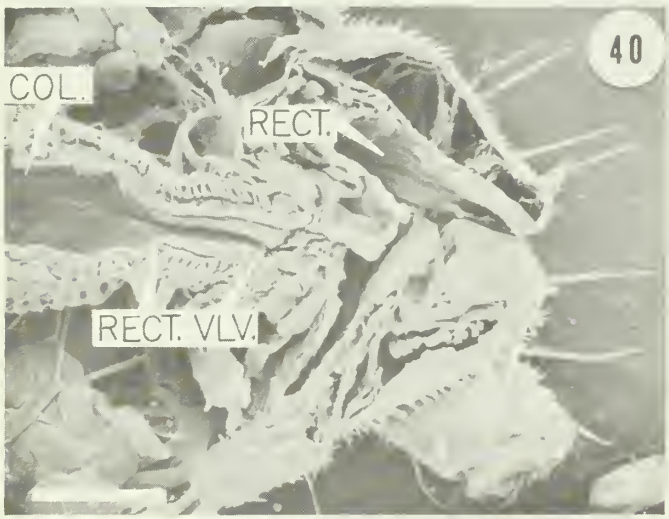

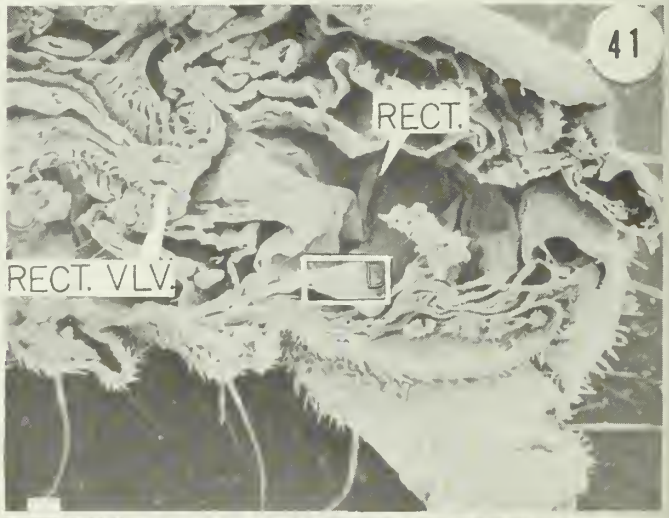

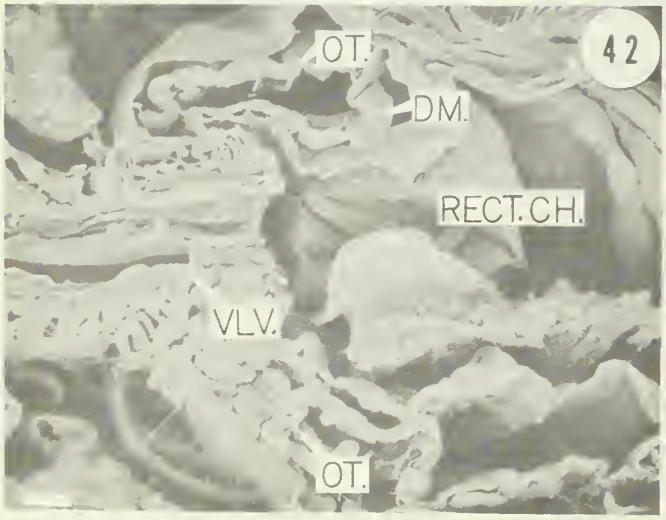

Figure 40. Sagittal section through the anal segments of late instar larva, the rectal chamber collapsed. COL, colon; RECT, rectum; RECT VLV, rectal valve. Bar = 1 mm. Figure 41. Similar section, with rectal chamber distended. RECT, rectum; RECT VLV, rectal valve. Bar = 100 . Inset is area shown in Fig. 43.

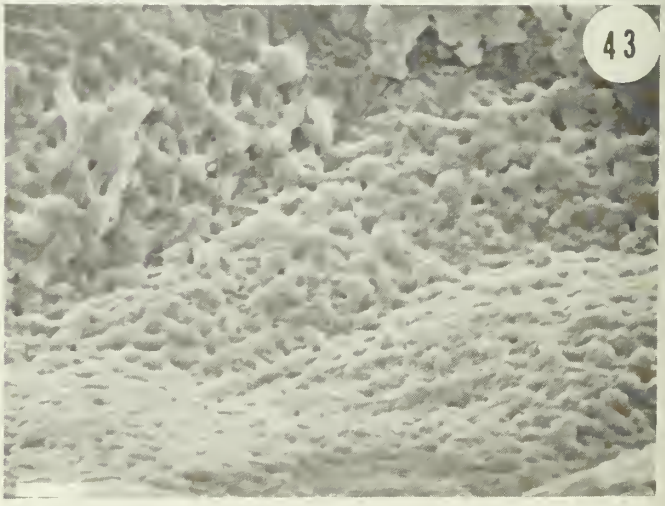

Figure 42. Close view of rectal valve, chamber, and cryptonephridic tubules. DM, double membrane separating inner and outer Malpighian tubules (inner tubules do not appear in this photo); OT, outer tubules; RECT CH, rectal chamber; VLV, rectal valve. Bar = 100 μm. Figure 43. Enlarged view of intima of rectal chamber, with irregular surface sculpture, and small micropores sprinkled over the surface. Bar = 1 μm.

Figure 44. Diagrammatic version of anal associations, with the colon collapsed. COL, colon; RECT, rectum; MT, malpighian tubules of the cryptonephridic system. Bar = 1 mm. Figure 45. Diagrammatic section of anal associations with the rectal chamber distended. RECT, rectum; V, rectal valve. Bar = 100 μm.

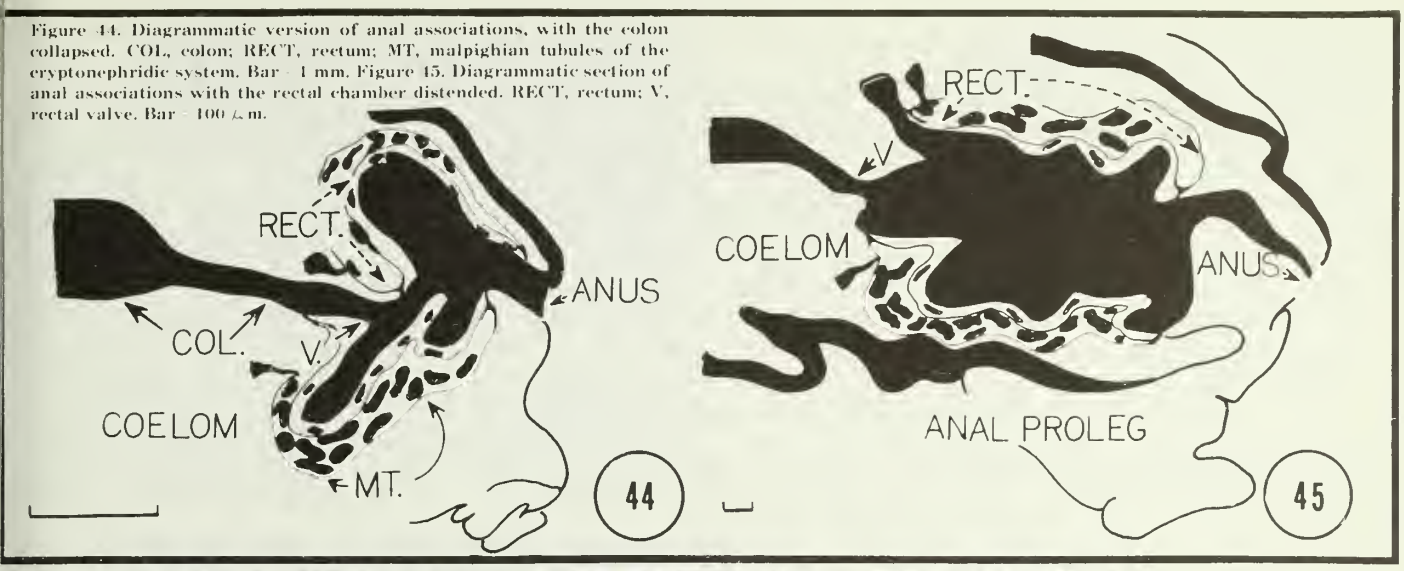

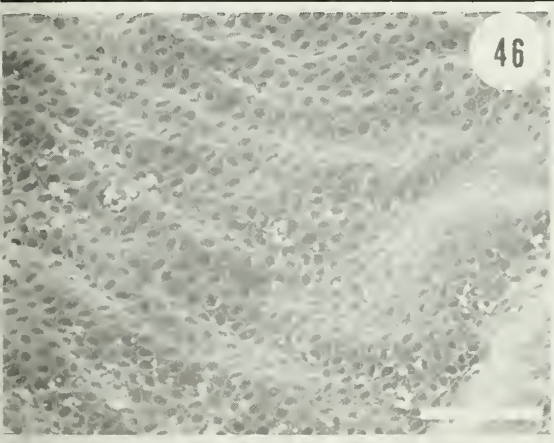

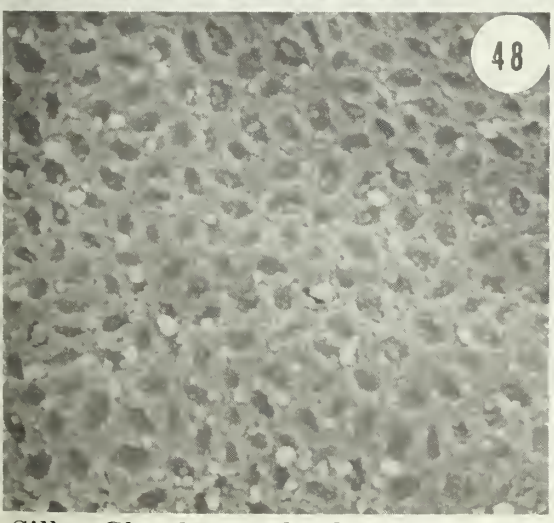

Figure 46. Epicuticular depressions of rectal intima at relatively low magnification (original at 4000X), depressions of ca. 1/2- 3/4 μm. densely scattered over the surface of the rectum, as well as the colon. Bar = 5 μm. Figure 47. Enlarged view of epicuticular depressions (original at 22300 X). Bar = 1 μm. Figure 48. View of epicuticular depressions, appearing as circular to oval pits, the borders and intervening areas granulate. Bar = 1 μm. Figure 49. External view of anal membranes, preserving roughly the 6-plicate pattern found throughout the hindgut. Anal membrane also bears the epicuticular depressions found in rectal intima. Bar = 100 μm.

Silk Glands and Salivary Glands (Figs. 50-55)

The large white silk glands (Figs. 50-55) are evident immediately upon opening the larvae. These originate at the silk press as fine ducts that lead to larger accessory glands (glands of Filippi, Fig. 54) that unite with the silk gland duct by two lateral channels. Silk glands are composed of an inner and outer duct throughout their length. The glands of Filippi have no distinct cell membranes and a diffuse nuclear material. The silk glands then progress caudad, fold beneath the crop and midgut and reemerge at about the middle of the midgut. The glands then form a sigmoid curve and terminate free in the coelom.

H. zea possesses a pair of small mandibular salivary glands (Fig. 1) as well as the silk glands. These extend to either side of the foregut

as transparent cones and narrow to very fine ducts beneath those of the silk glands.

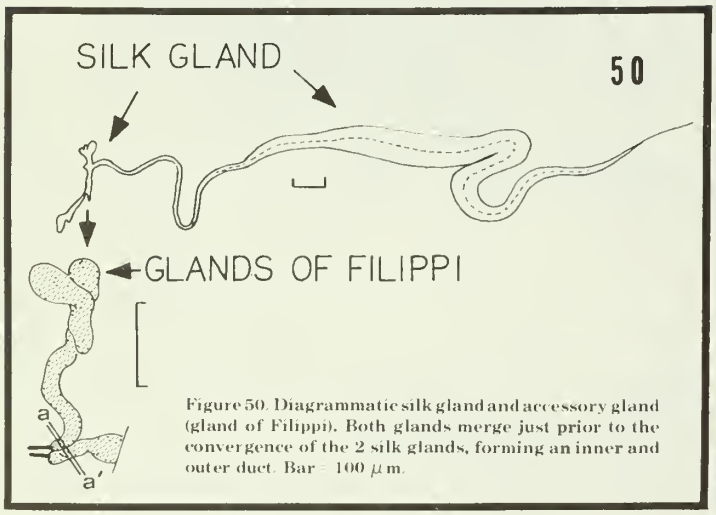

Figure 50. Diagrammatic silk gland and accessory gland (gland of Filippi). Both glands merge just prior to the convergence of the 2 silk glands, forming an inner and outer duct. Bar = 100 μm.

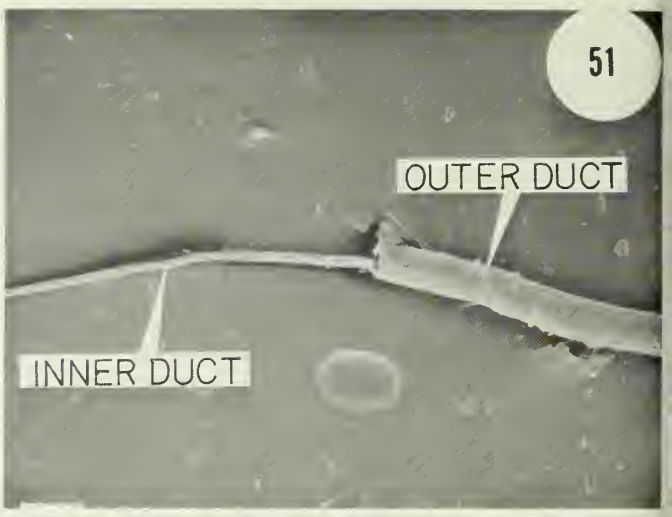

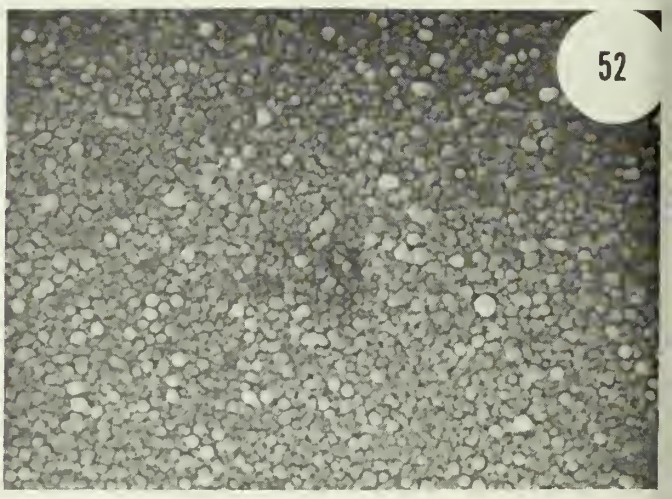

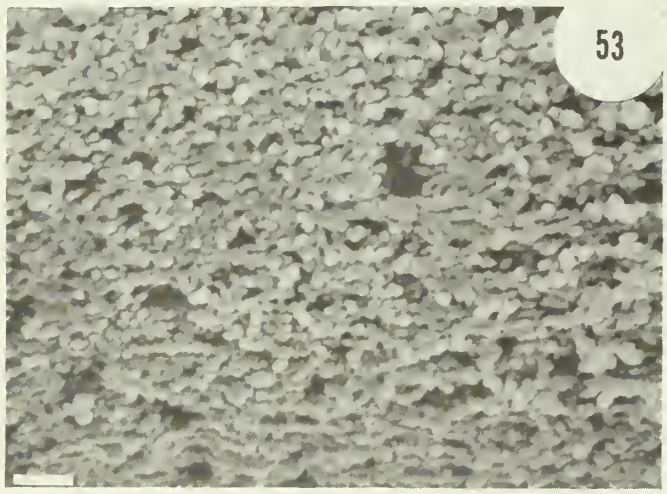

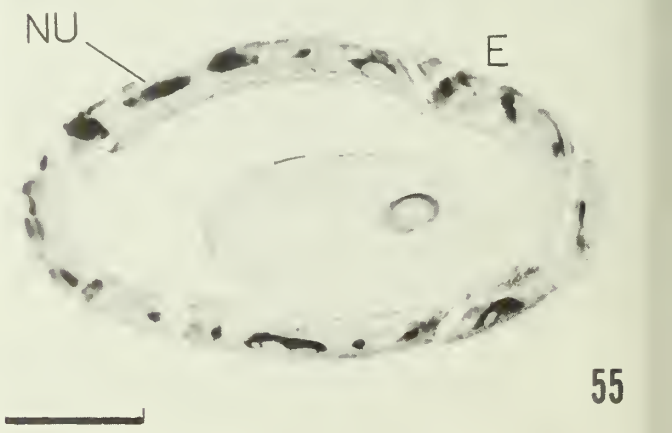

Figure 51. An inner duct or sheath runs through the outer main sheath of the silk gland. Bar = 100 μm. Figure 52. Topography of outer surface of inner sheath, showing a very finely granular surface at high magnification (original magnification 10,000 X). Bar = 1 μm. Figure 53. Coarser granularity of the surface of the outer sheath of the silk gland. This sheath has a cellular component, whereas the inner duct appears to be filled with viscid material. Bar = 1 μm. Figure 54. Cross section of silk gland conjoined with glands of Filippi, showing double walled tube. ID, inner duct; OD, outer duct. The section corresponds to a-a' of Fig. 50. The glandular aspect appears more or less amorphous, without true nuclear component or cell walls. Bar = 20 μm. Figure 55. Transverse section of silk gland, with inner, viscid mass, outer epithelium. NU, branched, elongate, or lobed nuclei characteristics of silk glands; E, epithelium.

Discussion

Several excellent papers have reported on the digestive systems of various lepidopterous larvae. Our study was not principally comparative, but certain observations can be related to those made on other species.

Judy and Gilbert (1970) reported specific dimensions for thickness of the foregut and hindgut intima of *Hyalophora cecropia*. We found this character to be quite variable. There may, however, be a terminal thickness in each instar. Measurements of intima thickness are very susceptible to nuances of sectioning because the intima is pulled easily from the underlying epithelium. Cell size also seems quite variable and often difficult to measure accurately because the cell membranes in fore and hindgut usually are obscure, even in well prepared specimens. Giant cells reported in the ileonodes may sometimes resolve into six or more smaller cells, but the apical cell usually is larger. Judy and Gilbert pointed out that the extrusion vesicles had cytoplasmic staining properties. This was true also of *H. zea*.

Anatomy of the hindgut is the most difficult to interpret, but the difficulty is resolved by using topographic information. Our observations on hindgut anatomy differ little from those of Reinecke et al (1973) for *Manduca sexta* or from Judy and Gilbert (1969-1970), but differ from the review by Byers and Bond (1971) because we recognize the ileum, which appears to be incorporated into the pylorus as they interpreted it. Also, the spicules of pyloric Pl-2 in *H. zea* are not hooked but are simply pointed, which may be a difference due to species. There is general agreement among these authors that the epicuticular depressions occur in the colon as well as in the rectum. However, none suggest that the depressions originate as micropores, as our photos show for both *Heliothis zea* and the boll weevil, *Anthonomus grandis* Boheman (MacGown and Sikorowski 1980).

References

Anonymous. 1976. Gill hematoxylin. Polysciences, Inc., Data Sheet No. 192. 4 pp.

Byers, J. R. and E. F. Bond. 1971. Surface specializations of the hindgut cuticle of lepidopterous larvae. Canadian J. Zool. 49:867-876.

Chapman, R. F. 1971. The Insects, Structure and Function. Elsevier publ. Co., N.Y. 819 pp.

Chauthani, A. R. and P. S. Callahan. 1967. Developmental morphology of the alimentary canal of *Heliothis zea* (Lepidoptera: Noctuidae). Annals Entomol. Soc. Amer. 60: 1136-40.

Chi, C. E., W. A. Drew, J. H. Young, and M. R. Card. 1975. Comparative morphology and histology of the larval digestive system of two genera of Noctuidae (Lepidoptera): *Heliothis* and *Spodoptera*. Annals Entomol. Soc. Amer. 68: 371-80.

Gurr, E. 1962. Staining, practical and theoretical. Williams and Wilkins Co., Baltimore. 631 pp.

Humason, G. L. 1967. Animal tissue techniques. W. H. Freeman and Co., N.Y. 569 pp.

Judy, K. J. and L. J. Gilbert. 1969. Morphology of the alimentary canal during metamorphosis of *Hyalophora cecropia* (Lepidoptera: Saturniidae). Annals Entomol. Soc. Amer. 62: 1438-1446.

_____ . 1970. Histology of the alimentary canal during metamorphosis of *Hyalophora cecropia* (L.). J. Morph. 131: 277-300.

MacGown, M. W. and P. P. Sikorowski. 1981. Digestive anatomy of the adult boll weevil, *Anthonomus grandis grandis* Boheman (Coleoptera: Curculionidae). Annals Entomol. Soc. Amer. 74: 117-126.

Reinecke, J. P., B. J. Cook, and T. S. Adams. 1973. Larval hindgut of *Manduca sexta* (L.) (Lepidoptera: Sphingidae). Int. J. Ins. Morph. and Embryol. 2: 277-290.

Saini, R. S. 1964. Histology and physiology of the cryptonephridial system of insects. Trans. Roy. Ent. Soc. London 116: 347-392.

Standlea, P. P. and T. R. Yonke. 1968. Clarification of the description of the digestive system of Heliothis zea. Annals Entomol. Soc. Amer. 61: 1478-81.

Mention of a trademark or proprietary product does not constitute a guarantee or warranty of the product by the Mississippi Agricultural and Forestry Experiment Station and does not imply its approval to the exclusion of other products that also may be suitable.